4.10 RESULTS FROM GLOBAL LAND-SURFACE DATA ASSIMILATION METHODS

Jon D. Radakovich[1], Paul R. Houser[2], Arlindo da Silva[3], and Michael G. Bosilovich[3]
[1] NASA Data Assimilation Office, General Sciences Corporation, Greenbelt, MD
[2] NASA Hydrological Sciences Branch, Greenbelt, MD
[3] NASA Data Assimilation Office, Greenbelt, MD

1. INTRODUCTION

Realistic representation of the land surface is crucial in global climate and weather prediction. Land-surface data assimilation techniques show significant potential to provide the required surface representation. In order to provide a test bed for land-surface data assimilation development, the Mosaic Land-surface Model (LSM; Koster and Suarez, 1992, 1996) has been driven off-line with GEOS-DAS (Goddard Earth Observing System Data Assimilation System) forcing, forming the Off-line Land-surface Global Assimilation (OLGA) system. This technique overcomes deficiencies in the original GEOS-1 DAS, where the soil moisture is prescribed, resulting in an imbalanced land-surface hydrologic budget. The OLGA system was also applied in conjunction with the assimilation of surface skin temperature observations.

2. METHODOLOGY

2.1 Mosaic LSM

The Mosaic LSM was chosen for use in OLGA because of its long history, sound theory, and community acceptance. Mosaic has its roots in the Simple Biosphere model developed by Sellers et al. (1986). Mosaic, however, captures sub-grid scale surface heterogeneity because each GCM grid point is divided into homogeneous tiles. Each tile represents a single vegetation or bare soil type. The tiles in a grid cell maintain independent energy and hydrology budgets, while the GCM responds to the area-weighted fluxes of heat and moisture from the tiles. Of course, such interaction is not present in OLGA.

2.2 OLGA System

In this study, the OLGA system was implemented globally at 2° x 2.5° resolution from 1981 through 1995 with GEOS-1 reanalysis atmospheric forcing. The data that drive OLGA are atmospheric temperature, specific humidity, downwelling shortwave and longwave radiation, surface pressure, and precipitation. The prognostic variables maintained in the Mosaic LSM include surface skin and deep soil temperature, the canopy vapor pressure, and the water content of the snow pack, interception reservoir, and three soil layers.

2.3 PSAS Temperature Assimilation

Another component of this study was the incorporation of PSAS (Physical-space Statistical Analysis System; Cohn et al., 1998) into OLGA, in order to assimilate surface skin temperature observations from ISCCP (International Satellite Cloud Climatology Project). The PSAS algorithm obtains the best estimate of the state of the system by combining observations with the forecast model first guess. The analysis equation, which encapsulates the PSAS scheme, is

$$w^a = w^f + K\left(w^o - Hw^f\right) \qquad (1)$$

where w^a denotes the analyzed field, w^f represents the model forecast first guess field, w^o is the observational field, K is the weights of the analysis, and H is the interpolation operator which transforms model variables into observables. In the OLGA (PSAS) framework, the grid space O – F (observed skin temperature minus the forecast first guess skin temperature) values are input to PSAS. PSAS retrieves a grid space average analysis increment ($\delta w^a = K(w^o - H\ w^f)$), that is transferred into OLGA tile space. The analyzed field is then obtained by adding the tile space analysis increment to the first guess skin temperature field.

2.4 Bias Correction

Preliminary results showed that simply correcting the OLGA skin temperature with the analysis increment from (1) every 3 hours was insufficient. Since w^f is biased, the traditional

[1] *Corresponding Author Address*: Jon D. Radakovich, General Sciences Corporation, Data Assimilation Office, NASA GSFC Code 910.3, Greenbelt, MD 20771, jrad@dao.gsfc.nasa.gov

analysis equation such as (1) produces a biased w^a (Dee and da Silva, 1998). Therefore, a variant of the Dee and da Silva (1998) bias correction (BC) scheme was implemented where,

$$\delta w^a = K\left(w^o - Hw^f + b^f\right) \quad (2)$$

$$w^a = w^f - b_{k-1}{}^f + \delta w^a \quad (3)$$

$$b_k{}^f = b_{k-1}{}^f - \gamma \cdot \delta w^a \quad (4)$$

$b_k{}^f$ is the updated bias estimate, $b_{k-1}{}^f$ is the bias estimate based on the previous analysis increment ($\delta w_{k-1}{}^a$) and δw^a is the analysis increment at time t_k. This scheme was inadequate because the bias generation mechanism associated with the surface skin temperature acted very quickly. As a result, an incremental BC scheme was introduced, where a BC term is added to the skin temperature tendency equation at every timestep to counteract the subsequent forcing of the analyzed skin temperature back to the initial state. For this scheme, b^f is computed as in (3) and the BC term is calculated as,

$$f_b = \frac{b^f}{\tau}. \quad (5)$$

where τ = 3 h is the frequency of the ISCCP dataset, i.e. the frequency of assimilation. This scheme effectively removed the time mean bias, but did not remove bias in the mean diurnal cycle. To account for this deficiency, we modeled the time-dependent bias as,

$$b^f(t) = \sum_j (a_j \cos\omega_j t + b_j \sin\omega_j t), \quad (6)$$

and estimated the Fourier coefficients

$$a_j = a_j - \gamma\delta w^a \cos\omega_j t \quad (7)$$

$$b_j = b_j - \gamma\delta w^a \sin\omega_j t. \quad (8)$$

We determined that at a minimum it is necessary to keep diurnal (ω_1=2π/24h) and semi-diurnal (ω_2=2π/12h) harmonics.

3. RESULTS

The results presented here are based on the evaluation of the discussed techniques for a July 1992 ISCCP surface skin temperature dataset. The test runs (Table 1) include the OLGA simulation without assimilation or BC (Model), OLGA with PSAS temperature assimilation (Assimilation I; Equation 1), OLGA with BC (Assimilation II; Equations 2-4), OLGA with incremental BC (Assimilation III; Equation 5), OLGA with diurnal BC (Assimilation IV; Equations 6-8) and OLGA with semi-diurnal BC (Assimilation V). Figure 1 shows the July 1992 global monthly mean standard deviations of surface skin temperature between the experiments and the observations. The standard deviation decreases gradually with each successive improvement to the methodology, and therefore substantiates the techniques developed. However, the standard deviation does not show the whole story because the impact of the diurnal BC is most visible in the monthly mean diurnal cycle.

Table 1: Description of experiments.

Experiment	Description
Model	OLGA Simulation
Assimilation I	OLGA with PSAS assimilation
Assimilation II	OLGA with BC every 3 h
Assimilation III	OLGA with incremental BC
Assimilation IV	OLGA with diurnal BC
Assimilation V	OLGA with semi-diurnal BC

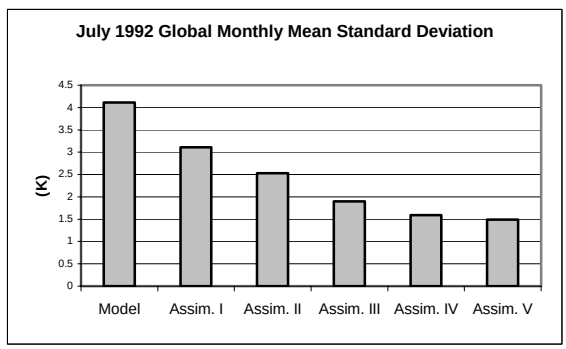

Figure 1: The July 1992 global monthly mean standard deviations of surface skin temperature between the OLGA experiments and the ISCCP observations (Table 1).

The July 1992 monthly mean diurnal cycle of surface skin temperature over North America for the ISCCP observations, Model, Assimilation IV, and Assimilation V, are presented at the top of Figure 2. The effectiveness of implementing semi-diurnal BC is shown by how closely Assimilation V matches the observations. Two meter temperature (middle) and specific humidity (bottom), also displayed in Figure 2, reveal that the inclusion of the BC scheme also impacts the surface meteorology fields. And so, for a decrease in surface skin temperature, due to BC, there is a corresponding decrease in the 2 m temperature and specific humidity. Figure 2

allows only for model intercomparison, and we are in the process of obtaining a verification dataset.

Similarly, the same corrective effect is visible in the Western Europe surface skin temperature for Assimilation V (Figure 3). The sensible heat flux (middle) and latent heat flux (bottom) also show that the BC technique has a substantial impact on the energy budget, where the reduction in skin temperature causes a decrease in the sensible and latent heat flux.

4. SUMMARY

In this study, the Mosaic LSM (Koster and Suarez, 1992, 1996) has been driven off-line with GEOS-DAS atmospheric forcing forming the OLGA system. PSAS was integrated into OLGA in order to assimilate three hourly ISCCP surface skin temperature data. Bias correction techniques were developed since traditional analysis with PSAS of a biased forecast lead to a biased analysis. The bias correction (BC) algorithms that were evaluated included BC every 3 h, incremental BC every timestep, and BC to the mean diurnal and mean semi-diurnal cycle. The results for a July 1992 test case have shown that the semi-diurnal BC was most effective. The monthly mean diurnal cycle from the semi-diurnal BC experiment closely matched the diurnal cycle from the observations. Also, the semi-diurnal BC results show the lowest standard deviation for the global monthly mean between the experiment and the observations.

5. REFERENCES

Cohn, S. E., A. da Silva, J. Guo, M. Sienkiewicz, D. Lamich, 1998: Assessing the effects of data selection with the DAO Physical-space Statistical Analysis System. *Mon. Wea. Rev.*, **126**, 2913-2926.

Dee, D. P., and A. da Silva, 1998: Data assimilation in the presence of forecast bias. *Q. J. R. Meteorol. Soc.* **124**, 269-295.

Koster, R.D., and M. J. Suarez, 1992: Modeling the land surface boundary in climate models as a composite of independent vegetation stands. *J. Geophys. Res.*, **97**, 2697-2715.

Koster, R.D., and M. J. Suarez, 1996: Energy and water balance calculations in the Mosaic LSM, NASA Technical Memorandum No. 104606, vol. 9, Goddard Space Flight Center, Greenbelt, MD, 60 pp.

Sellers, P. J., Y. Mintz, Y. C. Sud, and A. Dalcher, 1986: A simple biosphere model (SiB) for use with general circulation models. *J. Atmos. Sci.*, **43**, 505-531.

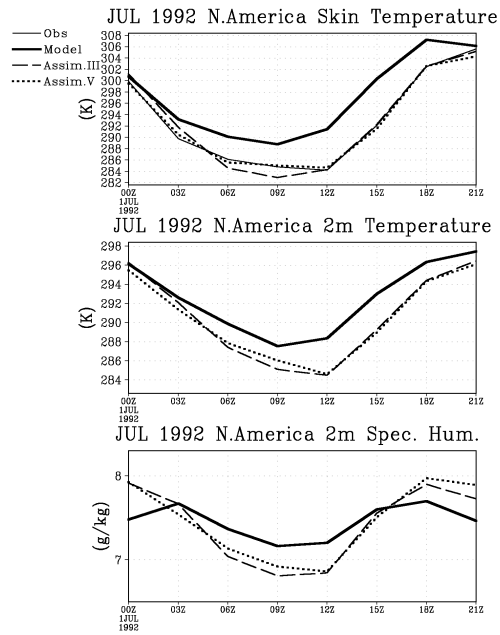

Figure 2. The July 1992 monthly mean diurnal cycle of skin temperature (top), 2 m temperature (middle) and 2 m specific humidity (bottom) over North America for the observations (light solid), Model (heavy solid), Assimilation III (dashed) and Assimilation V (dotted).

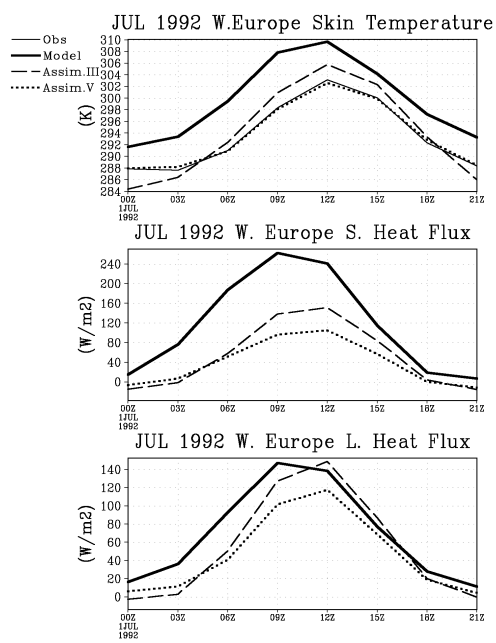

Figure 3. The July 1992 monthly mean diurnal cycle of skin temperature (top), sensible heat flux (middle), and latent heat flux (bottom) over Western Europe for the observations (light solid), Model (heavy solid), Assimilation III (dashed) and Assimilation V (dotted).